Hindawi
Wireless Communications and Mobile Computing
Volume 2022, Article ID 2796167, 12 pages
https://doi.org/10.1155/2022/2796167

Research Article

Intelligent Predictive Maintenance of Dry-Type Transformer Based on Vibration

Xiaoping Yang,[1,2] Xiao Zhao,[1,2] Xianhao Shen,[1,2] Yang Wang,[1,2] and Ce Xu[3]

[1]*School of Information Science and Engineering, Guilin University of Technology, Guilin, Guangxi 541004, China*
[2]*Guangxi Key Laboratory of Embedded Technology and Intelligent System, Guilin University of Technology, Guilin, Guangxi 541004, China*
[3]*Guilin Juntaifu Electric Company Limited, Guilin, Guangxi 541004, China*

Correspondence should be addressed to Xianhao Shen; 2120200988@glut.edu.cn

Received 14 July 2022; Revised 3 August 2022; Accepted 10 August 2022; Published 7 September 2022

Academic Editor: Kuruva Lakshmanna

The normal operation of the transformer is an important guarantee for the safe operation of the whole power network. Usually, the periodic maintenance work increases the workload of the operation and maintenance personnel. In this paper, an intelligent predictive and maintenance system for dry-type transformer based on vibration is proposed to monitor the vibration state of the transformer. The fractional-order Kalman filter and normalization method are used to preprocess the vibration data to reduce noise interference, and then the fault is classified by one-dimensional convolution neural network. On this basis, an improved grey Verhulst model is established to predict the fault time of the transformer. The experimental results show that the classification accuracy of the one-dimensional convolution neural network can reach more than 95%, and the improved grey Verhulst model can predict the fault of the dry-type transformer one week in advance.

1. Introduction

In recent years, with the expansion of China's power capacity, dry-type transformer, as an important component of the power system equipment, has received more attention. The normal operation of the transformer is an important guarantee for the safe operation of the whole power network. Due to the complex internal environment of the transformer, long-term work will produce various faults due to aging [1], which will seriously lead to regional power outages and safety accidents, threatening the property and life safety of the people. In order to eliminate the potential security risks of transformers [2] and reduce the economic losses caused by transformer damage and ensure life safety, predictive maintenance of transformers is needed.

At present, most domestic and foreign scholars still used the traditional machine learning algorithm to establish the dry-type transformer fault model and classify the state of the transformer. For example, C. Boonseng et al. [3] used neural network to classify and predict the state of transformer by axial acceleration, current, voltage distortion (THD), and current distortion (TDD). M. Bagheri et al. [4] mathematically modeled the vibration of transformer core and winding, established transformer vibration analysis model using vibration time series to analyze transformer abnormal and fault state, and then classified the vibration signal by BP neural network. The research on fault detection of dry-type transformer abroad has promoted the development of dry-type transformer detection technology in China to a certain extent. Cai Yonghua [5] used wavelet analysis method and convolution neural network method to analyze the vibration signal of transformer and proposes a transformer based on convolution neural network-based surface vibration signal feature extraction method. By monitoring the temperature, voltage, current, and other parameters of dry-type transformer system, Li Wang [6] established RBF (radial basis function) neural network to fit the nonlinear data to classify the state of winding and iron core. The vibration of dry-type transformer is not in a single direction when it fails. The traditional classification method of transformer

working state did not fully consider the acceleration of each direction of vibration, and there are problems such as complex processing steps, poor classification effect, and unable to predict the fault in advance.

In this study, the vibration information of the dry-type transformer is collected by the acceleration sensor ADXL356, and the fractional-order Kalman filter is carried out. The fault diagnosis of the vibration signal is carried out by one-dimensional convolution neural network. Finally, the grey Verhulst model designed can predict the fault time of the transformer one week in advance. The work done in this paper provides ideas and reference for the development of intelligent predictive maintenance technology of dry-type transformer, and has certain significance.

2. Experimental Details

2.1. Vibration Mechanism Analysis of Dry-Type Transformer. The main components of dry-type transformer are core and winding. Insulation pouring winding is wrapped on the core. The material of the core is usually laminated silicon steel sheet, which can effectively reduce the eddy current loss. The outer end of the winding is connected to the lead, which is responsible for the transmission of internal and external electric energy, and then the transformer ratio is controlled by the tap changer. The tap changer is also divided into two types: no-load tap changer and on-load tap changer. The difference between no-load tap changer and on-load tap changer is that the no-load tap changer needs to be powered off before adjusting the tap changer. The on-load tap changer can adjust the tap changer under the condition of power supply and change the transformer ratio by changing the winding turns of the transformer.

The iron core is often installed in the body through rigid connection parts. As shown in Figure 1, the vibration of the transformer is caused by the vibration of the iron core caused by Magnetostrictive [7] and Lorentz force [8], and the vibration of the winding affected by electromagnetic force applied to the load current. The vibration of the iron core and winding can be transmitted to the wall of the transformer through rigid connection components [9, 10].

2.1.1. Iron Core Fault. The core fault of dry-type transformer is mainly caused by core vibration and multi-point grounding, among which multi-point grounding is most likely to occur. The core failure is shown in Figure 2.

The iron core fault is mainly manifested as local overheating, abnormal vibration, and noise. The local overheating is generally caused by multi-point grounding and local short circuit. The multi-point grounding is often caused by the iron core contacting the transformer wall or the transformer entering the foreign body, which will lead to a rapid increase in the local temperature of the iron core [11]. The local short circuit may be caused by the aging of the insulating material. The abnormal vibration and noise are mainly caused by the loosening of the iron core caused by aging, which will cause winding deformation. According to statistics, the deformation at the top of the iron core is generally the most obvious. Therefore, sensors can be installed at the top of the transformer to collect vibration data.

2.1.2. Winding Fault. According to statistics, winding is the fault-prone point of transformer [12], mainly winding with vibration deformation caused by magnetic field force changes, winding aging, or not dry-type winding short circuit; winding fault can be shown in Figure 3.

Winding faults include winding short circuit and winding disconnection, which is generally caused by winding disconnection caused by poor welding. Winding short circuit is mainly caused by the decline of insulation capacity, including the aging of insulation materials, winding loose deformation caused by vibration, further leading to the overall vibration of the body.

2.2. Vibration and Fault Identification Method of Dry-Type Transformer

2.2.1. Vibration Data Acquisition. As shown in Figure 4, ADXL356C acceleration sensor produced by ADI Company is selected as the vibration sensor in this paper to monitor the vibration signal of SCB10-1600 wind power tower dry-type transformer and further monitor the state of the transformer. Place sensors to monitor the status of vulnerable areas, collect data every 0.1 seconds, and save them.

The sensor is placed at the bottom of the dry-type transformer to collect the vibration signal. When the transformer is under normal load, the rated current is applied to 92.4A, by applying 1.1 times rated current to simulate the fault. When the dry-type transformer is under normal load, the vibration acceleration range is between 0.6 m/s^2 when the rated current is applied. 1.1 times the rated current vibration range is between 0.7 m/s^2.

2.2.2. Vibration Data Process

(1) Data Filtering. In the application practice, the data collected by the sensor will have certain measurement errors, including the errors of the sensor system itself and the environment. The process of reducing noise interference is called filtering. Kalman filter estimation error mainly uses the minimum mean square error prediction model, which has good accuracy in noisy data. Kalman filter can estimate the equipment state at a certain time in the future through the current part of the model, so it is often used for data preprocessing.

Integer-order Kalman filter is mainly based on the estimated value of the previous moment to predict the state of the current moment, predict the covariance matrix of the error between the predicted value and the real value of the current moment, and then calculate the Kalman gain matrix of the current moment. The estimated value of the current moment can be updated by using the observed value of the current moment and finally update the covariance matrix of the error between the estimated value and the real value of the current moment [13, 14].

Considering that the noise in the actual engineering system may be non-Gaussian white noise, this paper uses the fractional-order Kalman filter [15] to effectively realize the state estimation of the continuous-time linear fractional-order system with fractional-order colored process noise or fractional-order colored measurement noise [16].

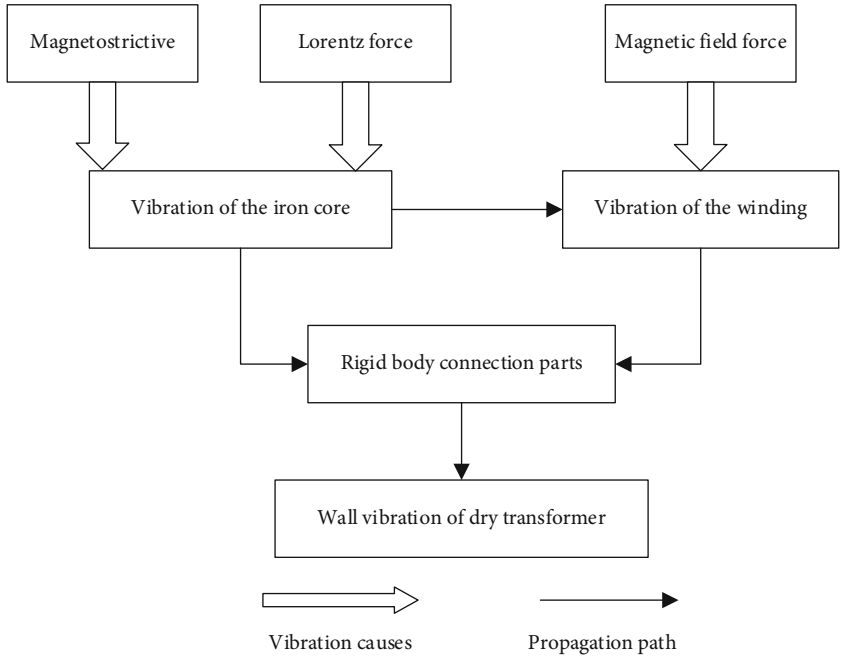

Figure 1: Vibration propagation diagram of dry-type transformer.

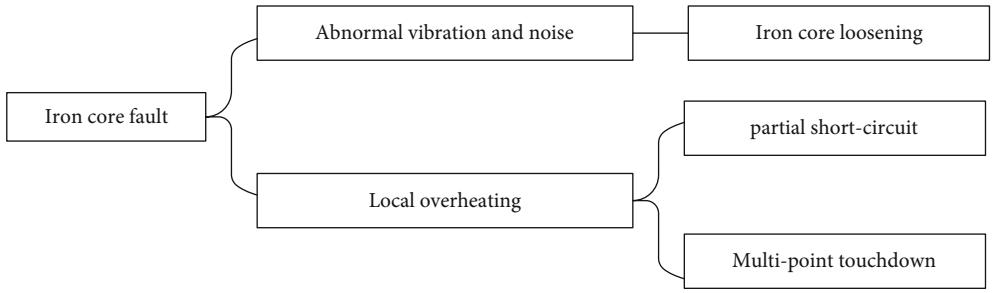

Figure 2: Iron core fault diagram.

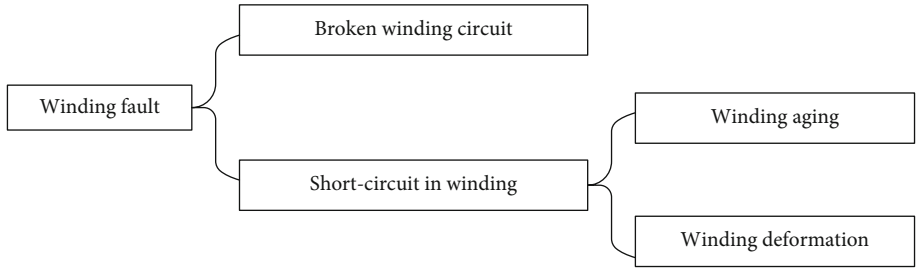

Figure 3: Winding fault diagram.

Combining fractional-order algorithm with Kalman filter, this paper will use the Grunwald-Letnikov definition of fractional discrete derivative:

$$\Delta^{\alpha} x_k = \frac{1}{h^n} \sum_{j=0}^{k} (-1)^j \binom{n}{j} x_{k+1-j}, \tag{1}$$

where n denotes the fractional order; h is the sampling interval; default is 1; h is the digital sample for calculating the derivative; and (n/j) can be expressed as:

$$\binom{n}{j} = \begin{cases} 1 & j = 0 \\ \dfrac{n(n-1)\cdots(n-j+1)}{j!} & j > 0 \end{cases}. \tag{2}$$

The state space model of fractional-order network

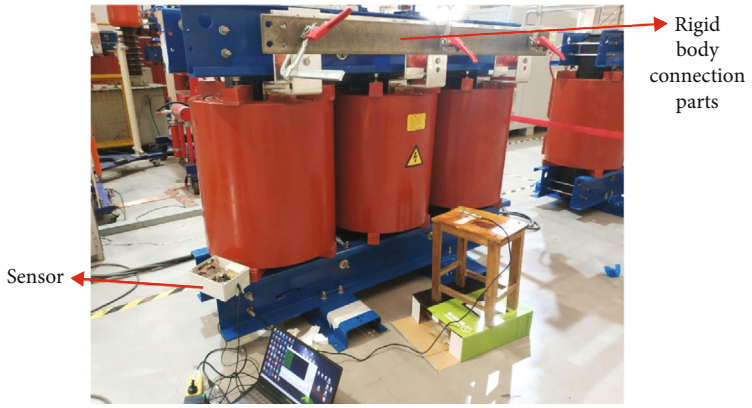

Figure 4: Field experiment.

system can be expressed by the following equation:

$$\begin{aligned} \Delta^{\propto} x_{k+1} &= A_d x_k + B u_k + w_k, \\ x_{k+1} &= \Delta^{\propto} x_{k+1} - \sum_{j=1}^{k+1} (-1)^j \propto_j x_{k+1-j}, \\ y_k &= C x_k + v_k, \end{aligned} \tag{3}$$

where A_d is the transition matrix, u_k is the system input, y_k is the system output, C is the output matrix, w_k is the system noise, and v_k is the instantaneous output noise:

$$\begin{aligned} \Delta^{\gamma} x_{k+1} &= \begin{bmatrix} \Delta^{n_1} x_{1,k+1} \\ \vdots \\ \Delta^{n_N} x_{N,k+1} \end{bmatrix}, \\ \gamma_k &= \operatorname{diag}\left[\begin{pmatrix} n_1 \\ k \end{pmatrix} \cdots \begin{pmatrix} n_N \\ k \end{pmatrix} \right]. \end{aligned} \tag{4}$$

Some related formulas are predefined:

$$\begin{aligned} \hat{x}_k &= \mathrm{E}[(x_k | y_k^*)], \\ \hat{P}_k &= \mathrm{E}\left[(x_k - \hat{x}_k)(x_k - \hat{x}_k)^T \right], \\ \tilde{x}_k &= \mathrm{E}[(x_k | y_{k-1}^*)], \\ \tilde{P}_k &= \mathrm{E}\left[(x_k - \tilde{x}_k)(x_k - \tilde{x}_k)^T \right], \end{aligned} \tag{5}$$

where $\hat{x}_k$ represents the state estimation variable, $\tilde{P}_k$ is the covariance matrix of estimation error, and $\tilde{x}_k$ is the state prediction matrix of time k. y_k^* is a measurement matrix, including the measured output $y_0, y_1, y_2, \cdots y_k$ and the input signal $u_0, u_1, u_2, \cdots u_k$. Usually, the conventional fractional Kalman algorithm can be mainly expressed by the following two steps:

Forecast equation:

$$\begin{aligned} \Delta^{\propto} \tilde{x}_{k+1} &= A_d \hat{x}_k + B, \\ \hat{x}_{k+1} &= \Delta^{\propto} \tilde{x}_{k+1} - \sum_{j=1}^{k+1} (-1)^j \propto_j \hat{x}_{k+1-j}, \\ \tilde{P}_{k+1} &= (A_d + \propto_1) \tilde{P}_k (A_d + \propto_1)^T + Q_k + \sum_{j=2}^{k+1} \propto_j P_{k+1-j} \propto_j^T. \end{aligned} \tag{6}$$

Filtering equation:

$$\begin{aligned} G_{k+1} &= \tilde{P}_{k+1} C^T \left(C \tilde{P}_{k+1} C^T + R_{k+1} \right)^{-1}, \\ \hat{x}_{k+1} &= \tilde{x}_{k+1} + G_{k+1} [y_{k+1} - C \tilde{x}_{k+1}], \\ \hat{P}_{k+1} &= (I - G_{k+1} C) \tilde{P}_{k+1}. \end{aligned} \tag{7}$$

G_{k+1} represents the Kalman filter gain vector at $k+1$. Q_k and R_k can be regarded as zero-mean Gaussian white noise with covariance matrix w_k and v_k. Q_k and R_k can be defined as:

$$\begin{aligned} Q_k &= E\left[w_k w_k^T \right], \\ R_k &= E\left[v_k v_k^T \right]. \end{aligned} \tag{8}$$

The vibration data after fractional Kalman filtering are shown in Figure 5. By comparing Figures 6 and 7, it can be seen that the data after the improved fractional Kalman filter are smoother, which facilitates the downstream fault classification.

(2) Normalization. In order to improve the convergence speed and accuracy of the model, the original data measured by the vibration sensor are normalized after fractional-order Kalman filtering.

$$\operatorname{norm}(x_i) = \frac{x_i - u_i}{\sigma_i}. \tag{9}$$

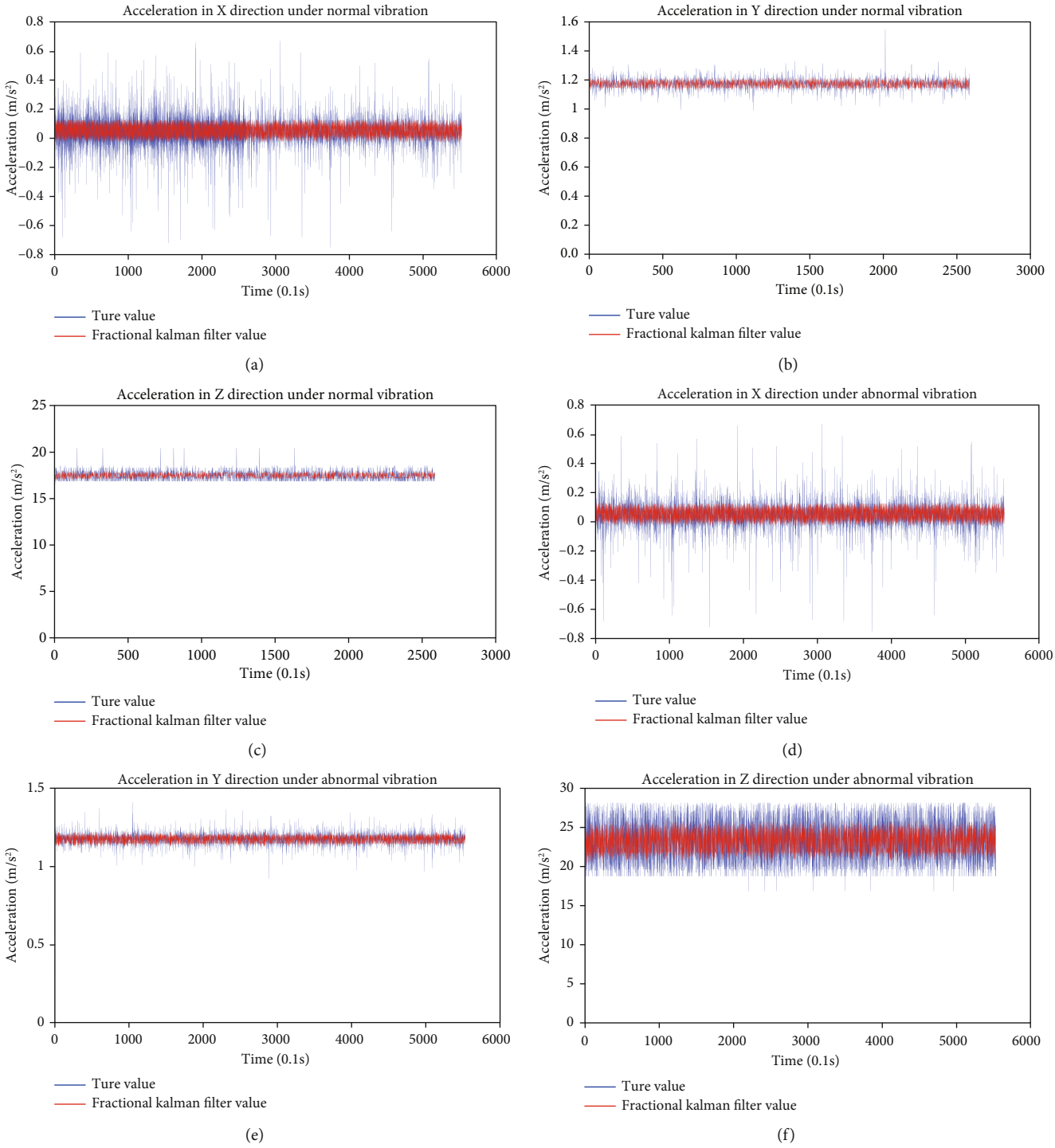

Figure 5: Fractional Kalman filtering results.

In the formula u_i and σ_i represent the mean and variance of group i data in the filtering sensing data. The zero-mean data of training set and test set are normalized and linearly scaled to [−1, 1]. The data obeys standard normal distribution, which is convenient for classification.

2.2.3. Fault Diagnosis Using One-Dimensional Convolutional Neural Network

(1) Dataset Partitioning. The state of the dry-type transformer will change when the transformer fails, so the state of the transformer can be judged by monitoring the vibration acceleration of the dry-type transformer.

In this paper, the whole working process of the transformer is divided into two stages: the stable working stage (the stable stage) and the fault warning stage (the warning stage). Then, for the normalized data, the above two labels

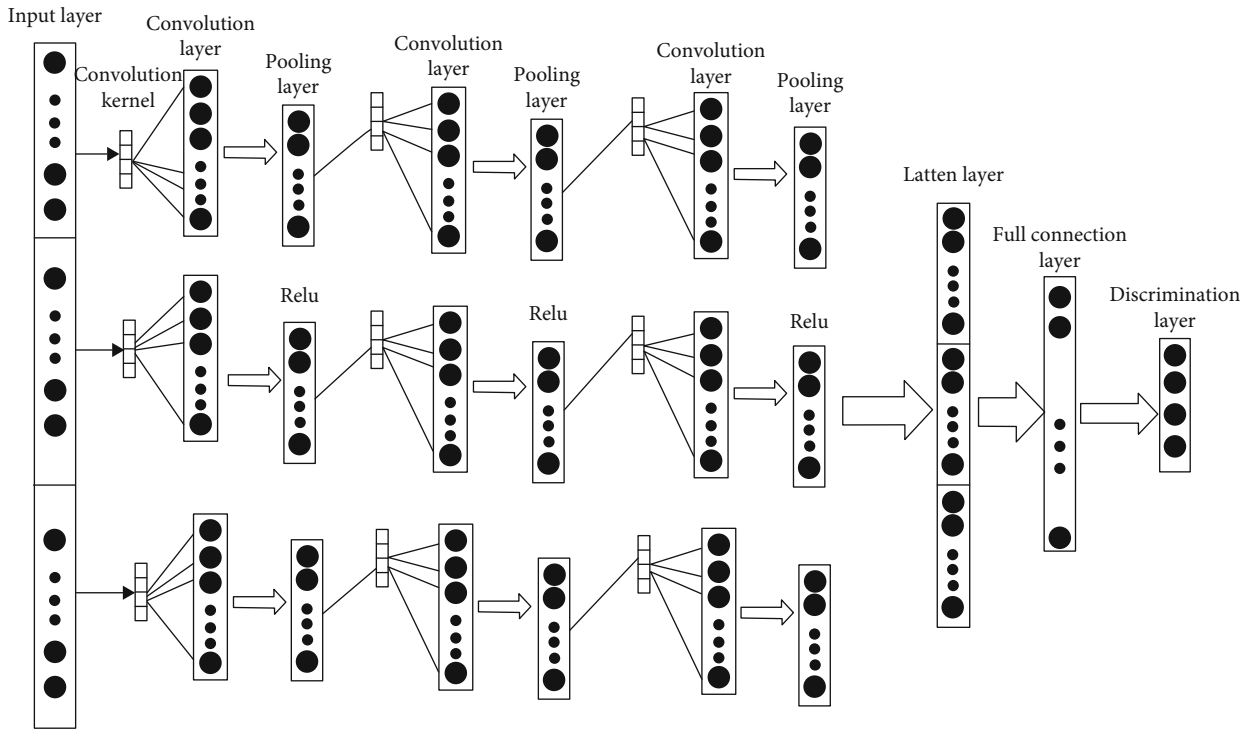

Figure 6: 1D-CNN network structure diagram.

are affixed to mark the data. Use 70% of the dataset as a training set and 30% as a test set.

(2) Design of Convolution Neural Network for Vibration Acceleration. 1D-CNN [17] (one-dimensional convolution neural network) is essentially the same as convolution neural network. Traditional CNN is mainly used for two-dimensional image recognition. The vibration acceleration of the transformer is a time series signal. If the time series signal is transformed into a binary image to process, it is easy to lose the fault information and miss the equipment fault. Therefore, the time series signal can be processed by one-dimensional convolutional neural network [18].

The 1D-CNN model was trained using the Keras framework in PyCharm software. The number of batch processing was 64, and epochs was 150. The loss function adopted the cross entropy loss function, and the SGD optimization algorithm was used. The learning rate was set to 0.001. The convolution kernel of the convolution layer is set to 4 and the step length is 1. The activation function of each convolution layer is selected as the Relu function. The convolution kernel of the pooling layer is set to 2 and the step length is 2. After two to three convolution layers and pooling layer operations, the pooling layer of the last layer is flattened by the flatten layer to obtain the full connection layer [19]. Finally, the softmax classifier is used for classification. This paper constructs a 9-layer 1D-CNN model, as shown in Figure 6.

2.3. Fault Prediction of Dry-Type Transformer. With the aging of the transformer, the service life is also continuously reduced. How to predict the fault at a certain time in the future at the beginning of the fault, that is, to predict the fault, can be realized by predicting the vibration data of the transformer. Therefore, it is an essential step to predict the vibration data of the transformer in the research of transformer fault prediction and maintenance. This paper studies and compares the grey GM (1,1) model and the grey Verhulst model [20]. The improved grey Verhulst model is applied to the prediction algorithm, which can predict the data well. The predicted data can be used to determine the fault by the above 1D-CNN model.

2.3.1. Pretreatment of Raw Data. In the original data, the previous data have a weak impact on the prediction effect of the prediction model, and the new information is often more representative of the change trend [21]. Therefore, we can remove $X^{(0)}(1)$ and increase $X^{(0)}(k+1)$ to obtain the new original data:

$$X^{(0)}(k) = x^{(0)}(2), x^{(0)}(3), \cdots, x^{(0)}(k+1). \tag{10}$$

Since the prediction model conforms to the law of exponential growth, it is necessary to smooth the original data. In this paper, the sliding smoothing method is used to process $X^{(0)}(k)$[17]. As follows:

$$X^{(0)}(k) = \left[x^{(0)}(k-1) + 2x^{(0)}(k) + x^{(0)}(k+1)\right]/4 \, (1 < k < n). \tag{11}$$

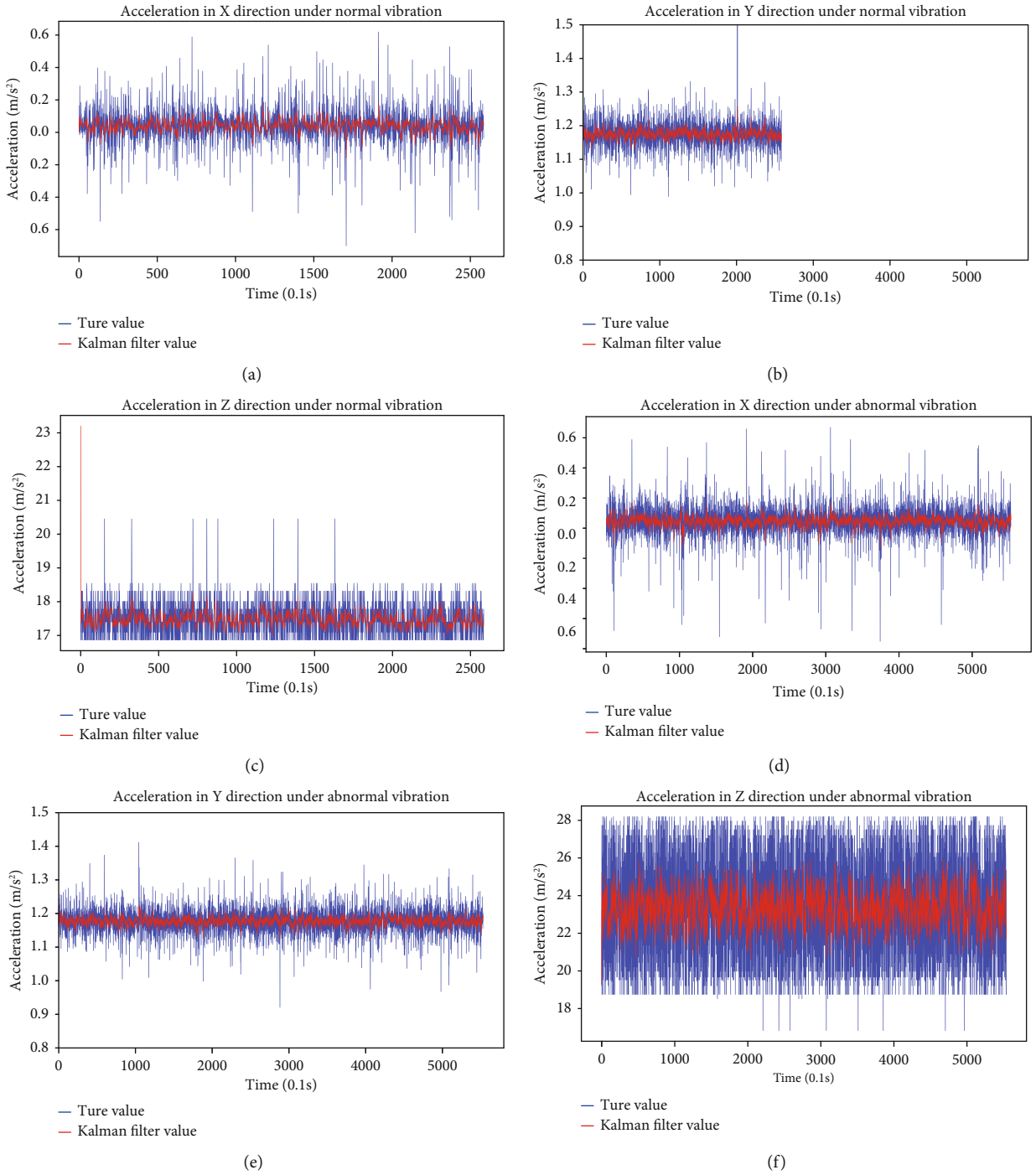

Figure 7: Integer-order Kalman filtering results.

Left and right endpoints can be expressed as follows:

$$X^{(0)}(1) = \left[3x^{(0)}(1) + x^{(0)}(2)\right]/4,$$
$$X^{(0)}(n) = \left[x^{(0)}(n-1) + 3x^{(0)}(n)\right]/4. \quad (12)$$

Through the establishment of the traditional grey Verhulst model, the background weight coefficient μ is also optimized. The traditional weight coefficient μ is defaulted to 0.5, but it is not necessarily the most suitable weight coefficient for the application object. On the basis of $\mu = 0$, a small amount of $\Delta\mu$ can be added, from 0 to 1, and the highest prediction accuracy of the model can be obtained [22], which is regarded as the best weight coefficient.

2.3.2. Background Value-Simpson Algorithm Design. $Z^{(1)}(k) = (x^{(1)}(k) + x^{(1)}(k-1))/2, k = 2, 3, \cdots, n$ is the background value in traditional prediction model. It is constructed by the trapezoidal formula in the numerical integration, not

necessarily the most suitable background value. According to the characteristics of the exponential function itself, the background value of the data is reconstructed by using Simpson's law, which is closer to the real data curve. The background value can be expressed by the following formula:

$$Z^{(1)}(k) = \frac{\left(x^{(1)}(k) + 4x^{(1)}(k-1) + x^{(1)}(k-2)\right)}{6}, k = 2, 3, \cdots, n. \tag{13}$$

3. Results

3.1. Data Filtering

3.1.1. Integer-Order Kalman Filter. The integer-order Kalman filter is used for filtering the vibration accelerations in X, Y, and Z directions under normal and abnormal vibrations. The filtering results are shown in Figure 7.

3.1.2. Fractional Kalman Filter. As shown in Figure 5, when we used the fractional-order Kalman filter for filtering the vibration accelerations in X, Y, and Z directions under normal and abnormal vibrations, the results show that the data becomes smoother. Smoother filtering results can effectively prevent the misjudgment of the neural network. This is because the vibration incentive of the transformer is complex and often presents an irregular state. Sometimes the sudden violent vibration in a short time is not caused by the fault. Therefore, this filter can more effectively eliminate the vibration noise, rather than identify the instantaneous large amplitude vibration as a fault.

3.2. One-Dimensional Convolution Neural Network Fault Identification Results

3.2.1. Influence of Activation Function. In this paper, the filtered vibration data sets are tested by fault discrimination experiment, and the fault overall discrimination rates of activation functions Sigmoid, Tanh, and Relu in the training set are analyzed and compared. The test is shown in Figure 8. Through comparison.

3.2.2. Influence of Convolution Kernel Number. In the 1D-CNN discriminant model 1 designed in this paper, the convolution kernel size in the convolution layer is set to 4, the step length is 1, the initial number of convolution kernels in model 1 is set to 8, and model 2 is set to 16. The discriminant effect is compared. After three convolution and pooling layers, the data is flattened by flatten layer, and then the data is discriminated by the full connection layer. The network structure parameters are shown in Tables 1 and 2.

Under the premise that the number of convolution iterations of the model is fixed to 3 times, different fault discriminant models are established by setting different number of convolution kernels. Model 1 sets 8 convolution kernels, and model 2 sets 16 convolution kernels, respectively, for training, and then test the discriminant effect. The characteristic curves of iteration number and discriminant rate are established in the training set, as shown in Figure 9.

Through the experiment, it can be seen that with the increase of the number of iterations, the discriminant rate is rising. After comparison, it is found that model 2 has faster convergence speed, and model 2 has higher prediction accuracy than model 1, so model 2 is better than model 1. The number of convolution kernels set to 16 is more suitable for the fault diagnosis.

3.2.3. Influence of Iteration Times. Iterative number design refers to the number of convolutions and pooling of the model. The more convolutions, the more features can be extracted. However, it will also lead to excessive calculation and over-fitting of the system. The number of convolution pooling is generally 2-3 times. This paper compares the discriminant effect of one-dimensional convolution neural network model with two and three iterations. Two iterative structures are designed as shown in Table 3, and three iterative structures are designed as shown in Table 4.

Under the condition that the number of convolution kernels is set to 16, model 3 and model 4 are established with different iterations. Model 3 is set to be iterated twice, and model 4 is set to be iterated three times. Train separately, and then test the discriminant effect. The fault discriminant rates of model 3 and model 4 in the test set are shown in Figure 10.

Through this experiment, it can be seen that the state discrimination rate of three iterations is higher than that of two iterations in the test set, so model 4 is better than model 3. Iteration 3 times is more suitable for the fault diagnosis.

3.3. Grey Verhulst Model.

Because the vibration signal will increase greatly when the transformer is running fault, the grey Verhulst model can be established to predict the fault time of the transformer. The average weekly vibration acceleration of dry-type transformer is taken, and the data from the first week to the eighth week are taken as input. The vibration acceleration of the transformer in the ninth week predicted by the model in the eighth week is shown in Figure 11.

The grey Verhulst model predicts that the transformer will have a large vibration amplitude at the ninth week, that is, the vibration amplitude of the fault is reached. Therefore, the maintenance personnel can overhaul the transformer at the eighth week. At week 7, based on the original data, by comparing the prediction results of GM (1,1) model, traditional Verhulst model, and grey Verhulst model improved by background value-Simpson algorithm, it is found that only the improved Verhulst model can be closer to the original data. Therefore, our improved grey Verhulst model has more accurate data prediction effect.

4. Discussion

Since the beginning of the 21st century, the demand for energy is growing. Wind energy as a renewable energy, wind power generation technology has been paid more and more attention by all countries in the world. Dry-type transformer is an embedded booster substation in the wind power tower. Its normal operation is an

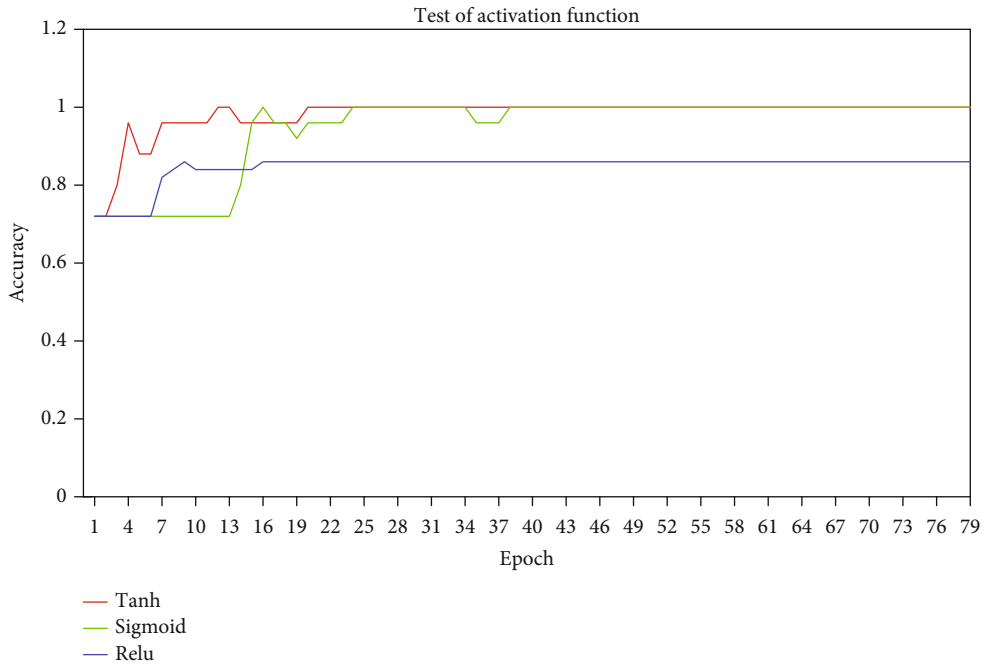

Figure 8: Test of activation function.

Table 1: One-dimensional convolutional neural network discriminant model 1 structural parameters.

Network structure	Convolution kernel size	Step size	Convolution kernel number	Output size
Convolution layer	4	1	8	64∗8
Pooling layer	2	2	8	32∗8
Convolution layer	4	1	16	32∗16
Pooling layer	2	2	16	16∗16
Convolution layer	4	1	32	16∗32
Pooling layer	2	2	32	8∗32
Flatten layer	256	1	—	256∗1
Fully connected layer	100-10-2	1	—	$100 * 1 - 10 * 1 - 2 * 1$
Discrimination layer	2	1	—	2∗1

Table 2: One-dimensional convolutional neural network discriminant model 2 structural parameters.

Network structure	Convolution kernel size	Step size	Convolution kernel number	Output size
Convolution layer	4	1	16	64∗16
Pooling layer	2	2	16	32∗16
Convolution layer	4	1	32	32∗32
Pooling layer	2	2	32	16∗32
Convolution layer	4	1	64	16∗64
Pooling layer	2	2	64	8∗64
Flatten layer	512	1	—	512∗1
Fully connected layer	100-10-2	1	—	$100 * 1 - 10 * 1 - 2 * 1$
Discrimination layer	2	1	—	2∗1

important guarantee for the safe operation of the whole power network. The fault of dry-type transformer is mainly aging problem, which is a long-term and slow process. However, the traditional machine learning algorithm does not have real-time and predictability to establish the fault model of dry-type transformer. Therefore, it is necessary to establish an accurate fault classification model, which is also the basis of fault prediction.

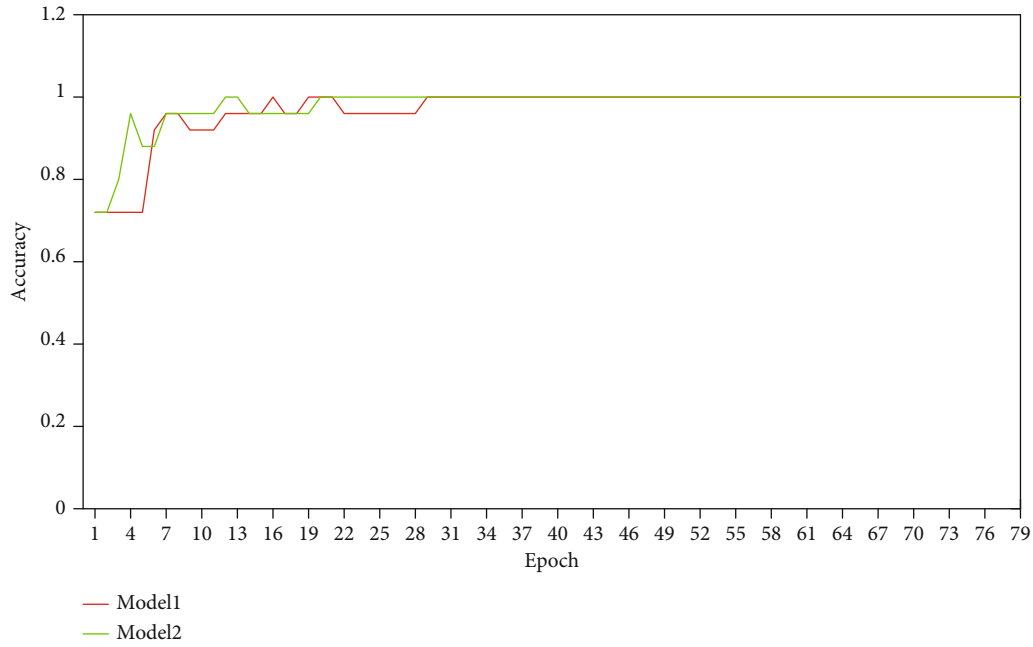

Figure 9: Test of kernel number.

Table 3: One-dimensional convolutional neural network discriminant model 3 structural parameters.

Network structure	Convolution kernel size	Step size	Convolution kernel number	Output size
Convolution layer	4	1	8	64∗8
Pooling layer	2	2	8	32∗8
Convolution layer	4	1	16	32∗16
Pooling layer	2	2	16	16∗16
Flatten layer	256	1	—	256∗1
Fully connected layer	100-10-2	1	—	$100 * 1 - 10 * 1 - 4 * 1$
Discrimination layer	2	1	—	4∗1

Table 4: One-dimensional convolutional neural network discriminant model 4 structural parameters.

Network structure	Convolution kernel size	Step size	Convolution kernel number	Output size
Convolution layer	4	1	8	64∗8
Pooling layer	2	2	8	32∗8
Convolution layer	4	1	16	32∗16
Pooling layer	2	2	16	16∗16
Convolution layer	4	1	32	16∗32
Pooling layer	2	2	32	8∗32
Flatten layer	256	1	—	256∗1
Fully connected layer	100-10-4	1	—	100∗1-10∗1-4∗1
Discrimination layer	4	1	—	4∗1

In this paper, the vibration signal of dry-type transformer is collected, and the data is filtered by a fractional-order Kalman filter. From the filtering results, this filter can make the vibration data smoother. Then, this paper proposes a 1D-CNN fault classification model with Tanh activation function, 16 convolution kernels, and three iterations through the 1D-CNN fault classification experiment using filtered data. The experimental data show that this model can achieve 100% recognition rate for dry-type transformer faults. Finally, the grey Verhulst prediction model is improved by background value-Simpson algorithm, and the effectiveness of the prediction model is demonstrated.

It is found that compared with the traditional machine learning algorithm, the neural network model can achieve

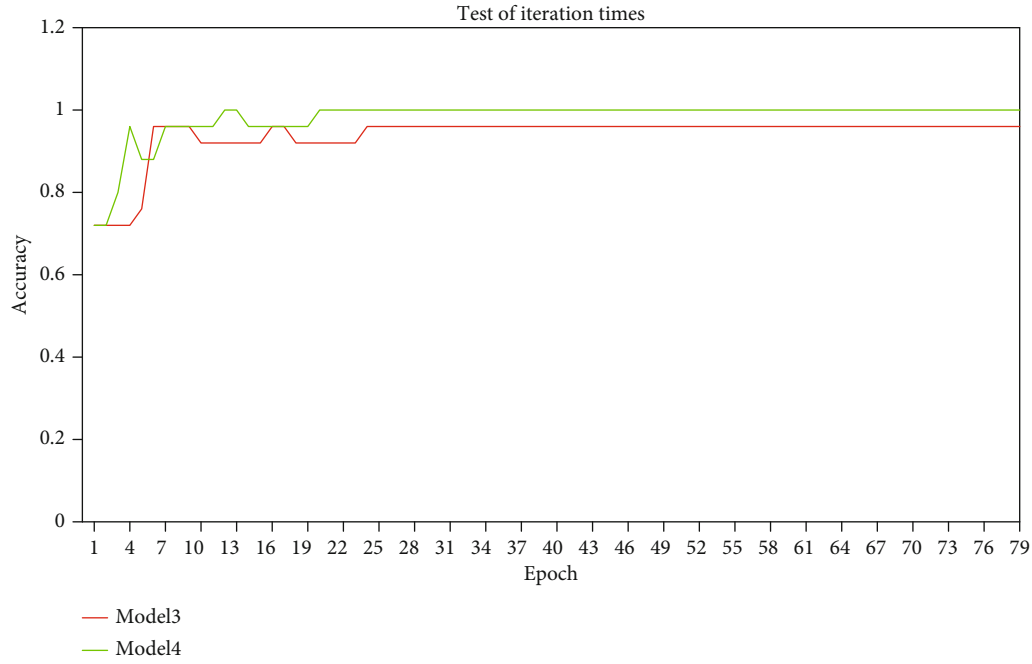

Figure 10: Test of iteration times.

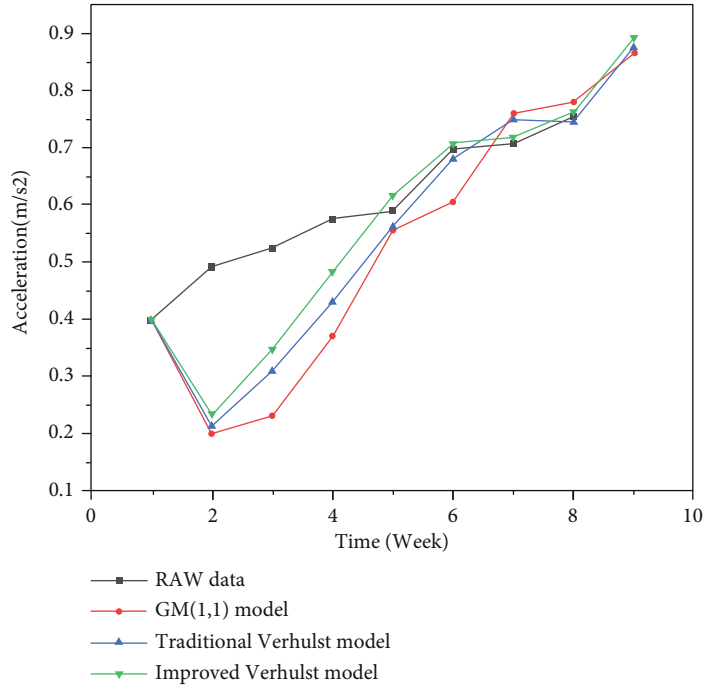

Figure 11: Data comparison diagram of prediction model.

more accurate fault identification results by learning a large number of vibration data in various directions. At the same time, the grey Verhulst prediction vibration fault prediction proposed in this paper makes up for the blank of dry-type transformer fault prediction.

However, due to the limitations of experimental conditions and cost, we used overcurrent input signal to simulate dry-type transformer's fault vibration and carry out filtering processing, fault classification, and prediction.

Therefore, in the future, we suggest that through long-term dry-type transformer condition monitoring, collect more transformer condition data to improve the database for future test analysis.

5. Conclusion

In this paper, the one-dimensional convolutional neural network is used to classify the equipment state with the filtering

data of fractional-order Kalman vibration data as input. The correct recognition rate of transformer fault is 95%. The experiment shows that with the increase of the number of convolution kernels and the number of iterations, it will have better discriminant effect, and Tanh activation function has good discriminant performance. The grey Verhulst model is also improved in this study. The results show that the prediction method can predict the fault of dry-type transformer one week in advance, and the basic functions of dry-type transformer prediction system can meet the design requirements. The following conclusions can be drawn from this study.

We can predict the dry-type transformer fault by vibration, especially using the fault identification and prediction method in this paper. However, there are still some areas that need to be improved and perfected, such as through long-term dry-type transformer condition monitoring, collecting more transformer state data to improve the database for future test analysis, and the intelligent predictive maintenance algorithm is applied to the local end to realize the local end fault warning.

Data Availability

The datasets used and/or analyzed during the current study are available from the corresponding author on reasonable request.

Conflicts of Interest

The authors declared no potential conflicts of interest with respect to the research, authorship, and/or publication of this article.

References

[1] R. M. A. Velásquez and J. V. M. Lara, "Root cause analysis improved with machine learning for failure analysis in power transformers," *Engineering Failure Analysis*, vol. 115, article 104684, 2020.

[2] W. S. Yuong, Y. Xiaofeng, F. Guo, and G. H. Hwang, "Computational intelligence for preventive maintenance of power transformers," *Applied Soft Computing Journal*, vol. 114, article 108129, 2022.

[3] C. Boonseng, R. Boonseng, and K. Kularbphettong, "Noise and vibration analysis of dry-type power transformer for monitoring and data mining applications," in *2019 22nd International Conference on Electrical Machines and Systems (ICEMS)*, pp. 1–5, Harbin, China, 2019.

[4] M. Bagheri, A. Zollanvari, and S. Nezhivenko, "Transformer fault condition prognosis using vibration signals over cloud environment," *IEEE Access*, vol. 6, pp. 9862–9874, 2018.

[5] C. Yonghua, "Analysis on transformer vibration signal recognition based on convolutional neural network," *Journal of Vibroengineering*, vol. 23, no. 2, pp. 484–495, 2021.

[6] L. Wang, "Research on fault diagnosis of mine dry-type transformer based on hybrid neural network WANG Li," *World Nonferrous Metals*, vol. 14, no. 2, pp. 177-178, 2019.

[7] X. Liu, J. Wu, F. Jiang, Y. Wang, C. Zhang, and Y. Hui, "Electromagneto-mechanical numerical analysis and experiment of transformer influenced by DC bias considering core magnetostriction," *Journal of Materials Science: Materials in Electronics*, vol. 31, no. 19, pp. 16420–16428, 2020.

[8] M. Wang, A. J. Vandermaar, and K. D. Srivastava, "Review of condition assessment of power transformers in service," *IEEE Electrical Insulation Magazine*, vol. 18, no. 6, pp. 12–25, 2002.

[9] X. C. Duan, Y. N. Li, L. J. Guo, Z. G. Zhao, and C. Li, "Finite element analysis of vibration characteristics of transformer core," *Control Engineering of China*, vol. 25, no. 6, pp. 1065–1070, 2018.

[10] P. Chao, X. Chen, and G. Cai, "Mode-state characteristics of three-phase unbalanced operation winding vibration of transformer based on electromagnetic mechanical coupling principle," *Proceedings of the CSEE*, vol. 40, no. 14, pp. 4695–4707 +4747, 2020.

[11] P. A. Wouters, A. van Schijndel, and J. M. Wetzer, "Remaining lifetime modeling of power transformers: individual assets and fleets," *IEEE Electrical Insulation Magazine*, vol. 27, no. 3, pp. 45–51, 2011.

[12] N. Li, H. Z. Ma, H. Zhu, J. Wang, J. J. Cui, and P. He, "Transformer winding looseness voiceprint recognition based on 50 Hz frequency multiplying wavelet time-frequency entropy and RUSBoost," *Electric Machines & Control Application*, vol. 49, no. 5, pp. 87–93, 2022.

[13] D. Peng, "Basic principle and application of Kalman filter," *Software Guide*, vol. 11, pp. 32–34, 2009.

[14] X. Li, K. Song, G. Wei, R. Lu, and C. Zhu, "A novel grouping method for lithium iron phosphate batteries based on a fractional joint Kalman filter and a new modified K-means clustering algorithm," *Energies*, vol. 8, no. 8, pp. 7703–7728, 2015.

[15] T. Liu, S. Cheng, Y. Wei, A. Li, and Y. Wang, "Fractional central difference Kalman filter with unknown prior information," *Signal Processing*, vol. 154, pp. 294–303, 2019.

[16] Y. Wang, Y. Sun, Z. Wei, and G. Sun, "State estimation of fractional order network system based on modified fractional order Kalman filter," in *2017 29th Chinese Control and Decision Conference (CCDC)*, pp. 112–116, Chongqing, China, 2017.

[17] S. Harbola and V. Coors, "One dimensional convolutional neural network architectures for wind prediction," *Energy Conversion and Management*, vol. 195, pp. 70–75, 2019.

[18] B. Wang, "Research on fault diagnosis method for hoist bearing based on one-dimensional convolutional neural network," *Mining & Processing Equipment*, vol. 49, no. 9, pp. 29–34, 2021.

[19] Y. Li, L. Zou, L. Jiang, and X. Zhou, "Fault diagnosis of rotating machinery based on combination of deep belief network and one-dimensional convolutional neural network," *Access*, vol. 7, pp. 165710–165723, 2019.

[20] J. Yang and X. Chen, "Application of Verhulst model in prediction of deformation of surrounding rock in roadway," *Industrial Minerals & Processing*, vol. 46, no. 12, pp. 41–43, 2017.

[21] X. Ang Li and D. J. Wang, "Prediction of foundation pit deformation near by the railway based on Verhulst dynamic metabolism," *Journal of Railway Science and Engineering*, vol. 14, no. 4, pp. 739–744, 2017.

[22] X. Wang, M. Zheng, and D. Zhang, "Application of improved GM (1, 1) model in landslide prediction," *Journal of East China Jiaotong University*, vol. 25, no. 4, pp. 11–14, 2008.

[23] Y. Ren, L. Li, N. Shi, and Y. Luo, "Application of improved GM (1, 1) model to dam deformation forecasting," *Engineering of Surveying and Mapping*, vol. 24, no. 6, pp. 61–64, 2015.